



# One-step green synthesis of $\beta$ -cyclodextrin/iron oxide-reduced graphene oxide nanocomposite with high supramolecular recognition capability: Application for vortex-assisted magnetic solid phase extraction of organochlorine pesticides residue from honey samples



Shokouh Mahpishanian, Hassan Sereshti\*

Department of Chemistry, Faculty of Science, University of Tehran, Tehran, Iran

## ARTICLE INFO

### Article history:

Received 23 August 2016

Received in revised form

12 December 2016

Accepted 12 January 2017

Available online 14 January 2017

### Keywords:

$\beta$ -Cyclodextrin

Graphene oxide

Gas chromatography

Organochlorine pesticides

Magnetic solid phase extraction

Honey

## ABSTRACT

In this research,  $\beta$ -cyclodextrin/iron oxide reduced graphene oxide hybrid nanostructure ( $\beta$ -CD/MRGO) with high water dispersability, excellent magnetic responsivity and molecular selectivity was prepared via a facile one step green strategy. The obtained nanomaterial was characterized by scanning electron microscopy (SEM), X-ray diffraction (XRD), Fourier transform infrared spectroscopy (FT-IR), Raman spectroscopy, and vibrating sample magnetometry (VSM), which confirmed the modification of GO with  $\beta$ -CD and magnetic nanoparticles. The formation mechanism of  $\beta$ -CD/MRGO was also discussed. The prepared magnetic nanocomposite was then applied as adsorbent in the vortex-assisted magnetic solid phase extraction (MSPE) of 16 organochlorine pesticides (OCPs) from honey samples prior to gas chromatography-electron capture detection (GC-ECD) analysis. Optimum extraction conditions have been assessed with respect to vortex time, sample pH, adsorbent amount, and salt concentration as well as desorption conditions (type and volume of desorption solvent and desorption time). A good level of linearity ( $2\text{--}10,000\text{ ng kg}^{-1}$ ) with satisfactory determination coefficients ( $R^2 > 0.9966$ ) and suitable precision (%RSDs less than 7.8) was obtained for OCPs under the optimal conditions. The limits of detection and quantification of the method were obtained in the sub-parts per trillion (ppt) to parts per trillion range (LOD:  $0.52\text{--}3.21\text{ ng kg}^{-1}$ ; LOQ:  $1.73\text{--}10.72\text{ ng kg}^{-1}$ ) based on 3 and 10 signal to noise ratios, respectively. The MSPE method was successfully applied to analysis of OCPs in honey samples with recoveries in the range of 78.8% to 116.2% and RSDs ( $n = 3$ ) below 8.1%. The results demonstrated that  $\beta$ -CD/MRGO could exhibit good supramolecular recognition, enrichment capability and high extraction recoveries toward OCPs.

© 2017 Elsevier B.V. All rights reserved.

## 1. Introduction

Organochlorine pesticides (OCPs) are one of the most effective compounds in the control of pests and diseases that have been widely used in agriculture around the world during the recent half century. But they have been listed as U.S. Environmental Protection Agency (EPA) priority pollutants [1]. The dangerous nature of OCPs is because of their toxicity, high chemical and biological stability and high potential to bio-accumulate [2]. Although, most of OCPs have been banned in many countries since 1970s, they are still found in the environment owing to their extreme stability. Furthermore, in many underdeveloping countries, OCPs are still used

due to the low cost and versatility in controlling a number of pests [3]. The adverse effects of OCPs as endocrine disruptors [4] or carcinogens [5] and low biodegradability make them a significant risk to human health and natural ecosystems. The accumulation of OCPs in animal-based products is another great concern because these products act as intermediates in the transport of pollutants from soil, plant, water and air to humans.

Honey is a valuable natural food product of animal origin with world-wide consumption and it should be free from any chemical contaminants according to the European Union (EU) regulations (74/409/EEC, 1974) [6]. Due to the persistence of OCPs in the environment, they may be introduced to honey during its production by bees when they come in contact with nectar and pollen from blossoms in lands where previously were exposed to pesticides. Therefore, the monitoring of pesticides residues in honey is an important issue in terms of food safety concern. Owing to com-

\* Corresponding author.

E-mail addresses: [sereshti@khayam.ut.ac.ir](mailto:sereshti@khayam.ut.ac.ir), [sereshti@ut.ac.ir](mailto:sereshti@ut.ac.ir) (H. Sereshti).

plex matrix of honey, efficient sample pretreatment is essential to obtain reliable results for trace level analysis. Several sample preparation techniques [7–13] have been reported for the extraction of pesticide residues from honey which among them, solid phase extraction (SPE) with different adsorbents has gained research interest. In spite of some benefits, traditional SPE suffers from several drawbacks such as limited rates of diffusion and mass transfer, cartridges blocking by matrices particles, difficulty to treatment of large sample volumes and adsorbing the analytes on the plastic wall of cartridges which may cause to decrease the recovery and increase the interferences in the analysis [6].

Magnetic solid phase extraction (MSPE) is a SPE-based methodology that has gained much attention in recent years. In this method, the sorbent is directly added into the sample solution containing the target analytes and collection of sorbent is easily carried out by an external magnetic field which greatly simplifies the SPE procedure and avoiding channeling or blocking of cartridges as occurs in traditional SPE [14]. Different magnetic materials can be applied as sorbents with MSPE. Recently, magnetic carbon nanostructures have attracted research interest as the adsorbent since they often exhibit a high adsorption capacity for different compounds [15]. Graphene oxide (GO) as a carbon nanomaterial, with the structure of a flat monolayer of carbon atoms bonded into a two-dimensional (2D) honeycomb lattice, reveals many interesting properties such as high mechanical, chemical and thermal stability, ease of functionalization, excellent water dispersability and high surface-to-volume ratio that make it an ideal choice for use as adsorbent [16]. The introduction of magnetic properties into GO will combine the extraordinary properties of GO and the separation convenience of the magnetic materials. Many efforts have been made in recent years to surface functionalization of graphene-based magnetic nanocomposites in order to improve the selectivity of the extraction system and achieve better adsorptive properties.

$\beta$ -Cyclodextrin ( $\beta$ -CD) is a cyclic oligosaccharide supramolecular composed of seven glucopyranose units. This compound contains an electron-rich hydrophobic cavity due to its carbon chain conformation and a hydrophilic exterior surface because of oriented the 21 hydroxy groups on the rims of the macrocycle [17]. The most extraordinary characteristic of  $\beta$ -CD is its ability to form inclusion complexes (host-guest complexes) by capturing various compounds with suitable polarities and dimensions into its cavity and therefore showing high molecular selectivity and enantioselectivity [18,19]. In addition,  $\beta$ -CD is environmentally friendly and water-soluble which can improve the solubility and dispersability of functional materials.

Based on the unique performances of GO and  $\beta$ -CD, the integration of them into a new composite synergically offers two materials individual benefits, such as large surface area of GO and high supramolecular recognition and enrichment capability of  $\beta$ -CD. Therefore, the  $\beta$ -cyclodextrin/graphene (graphene oxide) nanocomposites will provide potential applications in the many fields, especially organic pollutant separation and purification [20–24]. In recent years, researchers have exploited various strategies to fabricate cyclodextrin functionalized nanomaterials. In the previously reported methods, the preparation of  $\beta$ -cyclodextrin/graphene composites consisted of several time consuming steps that in some cases, the reducing agent used in the chemical reduction of GO was a hazardous material such as highly poisonous hydrazine [20,25–28]. The experiments showed that the synthesized magnetic nanocomposites functionalized with  $\beta$ -CD not only have the magnetic property of  $\text{Fe}_3\text{O}_4$  nanoparticles which make them easily manipulated by an external magnetic field, but also have the large surface area of GO that can incorporate high number of  $\beta$ -CD molecules [27,28].

In this work,  $\beta$ -CD/MRGO nanocomposite was successfully prepared by a simple one-step hydrothermal method using non-toxic

and cost-effective precursors. In this strategy, the reduction of GO to graphene, attachment of  $\beta$ -CDs molecules onto the GO nanosheets and the in situ deposition of  $\text{Fe}_3\text{O}_4$  nanoparticles were occurred in one step. Here in, the  $\text{Fe}^{2+}$  ions acted as reducing agent for reducing oxygen functional groups on the surfaces of GO nanosheets which is non-toxic. The synthesized  $\beta$ -CD/MRGO was then characterized by SEM, XRD, FTIR, VSM and Raman spectroscopy. Finally, the application of prepared nanocomposite as adsorbent for extraction of sixteen organochlorine from honey by a vortex-assisted solid phase extraction procedure was investigated. Fig. 1 illustrated the synthesis of  $\beta$ -CD/MRGO and different steps of OCPs extraction and analysis.

## 2. Experimental

### 2.1. Reagents and materials

Acetonitrile (HPLC gradient grade), acetone, *n*-hexane (Pestanal grade), dichloromethane, methanol, hydrochloric acid (HCl), sodium hydroxide (NaOH),  $\beta$ -cyclodextrin, sodium chloride (NaCl), ferrous sulfate heptahydrate ( $\text{FeSO}_4 \cdot 7\text{H}_2\text{O}$ ), ammonia solution ( $\text{NH}_3$ , 25%) and all other reagents were purchased from Merck Chemicals (Darmstadt, Germany). The OCPs were obtained as a commercial mixture (EPA 608 pesticide mix, stock standard solution of  $20 \mu\text{g mL}^{-1}$  each component in toluene:*n*-hexane, 1:1) from Sigma-Aldrich (St Louis, MO, USA). The mixture contained the following compounds:  $\alpha$ -HCH,  $\beta$ -HCH,  $\gamma$ -HCH,  $\delta$ -HCH, aldrin, dieldrin, endosulfan I, endosulfan II, endosulfan sulfate, endrin, endrin aldehyde, heptachlor, heptachlor epoxide-isomer B, *p,p'*-DDE, *p,p'*-DDD, and *p,p'*-DDT. Appropriate dilutions of the stock solution with distilled water were made to the working solutions.

All standard solutions were stored in a refrigerator at  $-4^\circ\text{C}$  in the dark. All laboratory glassware used in this study was washed with detergent, thoroughly rinsed with distilled water and acetone, and then heated to  $120^\circ\text{C}$  overnight to remove any remaining OCPs and contaminants on the surface of vials.

### 2.2. Instrumentation

Chromatographic analyses were carried out using a gas chromatograph Agilent 7890 (Santa Clara, USA) equipped with a micro electron capture detector ( $\mu$ -ECD). All the separations were performed on a HP-5 fused silica capillary column ( $30 \text{ m} \times 0.32 \text{ mm}$  i.d.  $\times 0.25 \mu\text{m}$ , film thickness; 5% phenyl-95% dimethyl siloxane) (Agilent Scientific, USA) with helium ( $>99.999\%$ ) as carrier gas at  $1.0 \text{ mL min}^{-1}$  flow-rate and nitrogen as make-up gas ( $30 \text{ mL min}^{-1}$ ). The injection port and detector temperature were set at  $250^\circ\text{C}$  and  $300^\circ\text{C}$ , respectively. An amount of  $1 \mu\text{L}$  of sample was injected in splitless mode, during 0.75 min. The column oven temperature program was as follows: initial temperature  $60^\circ\text{C}$  (held 1 min), increased at  $30^\circ\text{C min}^{-1}$  to  $180^\circ\text{C}$ , and then raised to  $250^\circ\text{C}$  at  $7^\circ\text{C min}^{-1}$  (held for 5 min).

FT-IR spectra were obtained on an Equinox 55 FT-IR spectrometer (Bruker, Bremen, Germany) from  $4000$  to  $400 \text{ cm}^{-1}$  using a KBr pellet. The morphology of the  $\beta$ -cyclodextrin/MRGO was observed using a Zeiss DSM-960 scanning electron microscope (SEM, Oberkochen, Germany). The magnetic properties of the prepared materials were studied using a vibrating sample magnetometer (VSM/AGFM Meghnatis Daghigh Kavir Co., Kashan, Iran) at room temperature.

X-ray diffraction (XRD) patterns were collected on a X'Pert Pro MPD X-ray diffractometer (Almelo, Netherlands) using a Cu-K $\alpha$  radiation ( $\lambda = 1.54178 \text{ \AA}$ ). Raman spectra were conducted on a SENTERRA Dispersive Raman microscope (Bruker, Germany) with a  $785 \text{ nm}$  wavelength incident laser light. The samples were vortexed

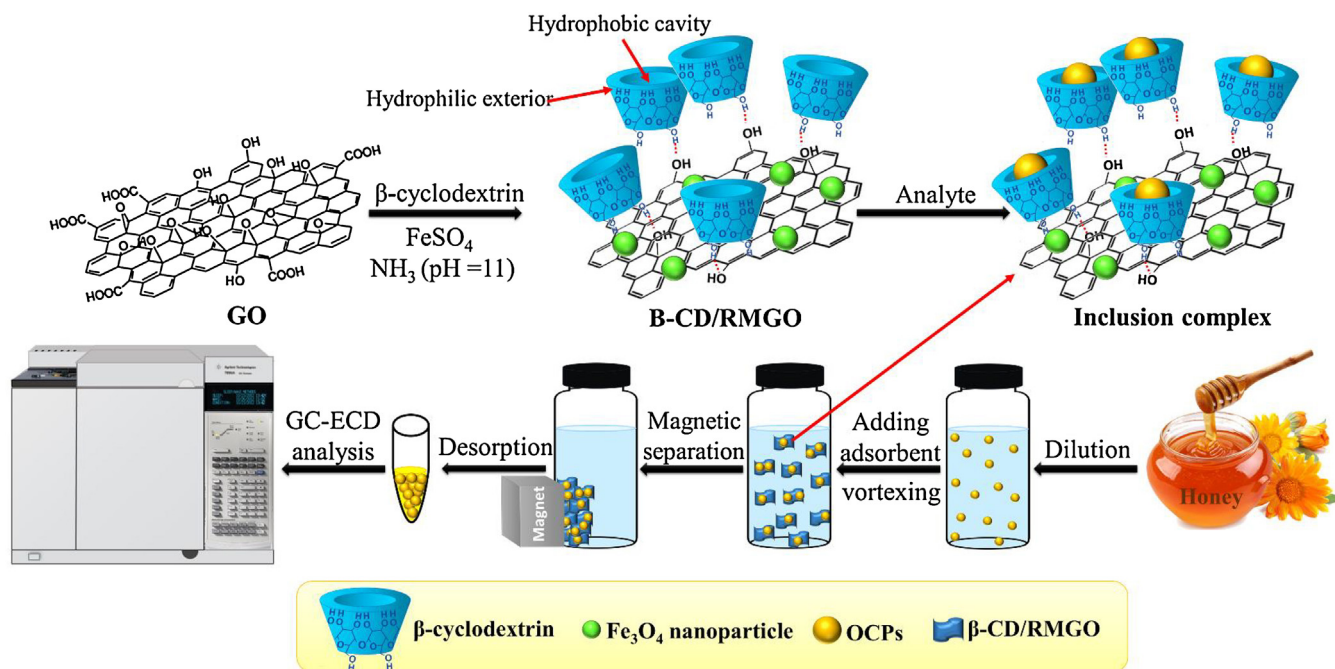


Fig. 1. Illustration of the procedure for synthesis of  $\beta$ -CD/MRGO and MSPE steps for OCPs analysis in honey.

utilizing A ZX-Classic vortex mixer (Velp Scientifica, Milan, Italy). A Eurosonic 4D (Euronda, Montecchio Precalcino (Vincenza) Italy) ultrasonic water was used in the synthesis of the adsorbent and the optimization procedure.

### 2.3. Synthesis of $\beta$ -CD/MRGO

The GO nanosheets were synthesized from natural graphite by a modified Hummers' method [29]. For fabrication of  $\beta$ -CD/MRGO, 0.250 g of  $\beta$ -CD and 0.695 g of  $\text{FeSO}_4 \cdot 7\text{H}_2\text{O}$  were added to the 50.0 mL aqueous dispersion of graphene oxide ( $2 \text{ mg mL}^{-1}$ ) and ultrasonicated for five min. Next, the pH of sample was adjusted to 11 by ammonia solution and the vial was placed in a water bath at  $60^\circ\text{C}$  for 5 h with constant stirring under  $\text{N}_2$  atmosphere. The resultant black dispersion was collected by a magnet, washed several times with ethanol and distilled water sequentially to remove excess  $\beta$ -CD, and then dried in vacuum at  $40^\circ\text{C}$  for 6 h.

Magnetic reduced graphene oxide (MRGO) was synthesized by the same procedure described above without addition of  $\beta$ -CD to the sample solution.

### 2.4. The MSPE procedure

The schematic MSPE procedure is shown in Fig. 1. Typically, 15 mg of  $\beta$ -CD/MRGO was added to 50 mL of the sample solution containing OCPs ( $500 \text{ ng kg}^{-1}$ ) in a glass tube. The tube was then shaken by vortex mixer for 3 min at 3000 rpm. After that, a magnet was placed on the outside wall of the tube to collect  $\beta$ -CD/MRGO nanoparticles which had adsorbed the analytes. After completing the separation of nanoparticles from the solution in a few seconds ( $< 30 \text{ s}$ ), the clear supernatant was discarded. Next, the residual supernatant and adsorbent were completely transferred to a 2 mL centrifuge tube and the adsorbent was collected again by placing a magnet to the outside of tube wall to completely remove the residual OCPs from the solution. In the next step, the analytes were desorbed from the adsorbent by vigorous vortexing the mixture with 0.5 mL of mixed solvent system containing acetonitrile and dichloromethane (4:1, v/v) for 1 min. This desorption procedure

was performed one more time. The desorbed solutions were then combined together and evaporated to dryness under a mild stream of nitrogen at  $40^\circ\text{C}$ . The residue was redissolved in 100  $\mu\text{L}$  of *n*-hexane, and 1  $\mu\text{L}$  of it was injected into the GC- $\mu\text{ECD}$  to analyze.

### 2.5. Statistical analysis

The statistical analyses were carried out using SPSS 15.0 for windows (SPSS Inc., Chicago, IL, USA). The obtained data were compared for any significant differences using one-way analysis of variance (ANOVA) and Tukey Comparisons Test. Differences at probability level of 95% ( $P < 0.05$ ), considered to be significant.

## 3. Results and discussion

### 3.1. Characterization of $\beta$ -cyclodextrin/MRGO

The FT-IR spectra of  $\beta$ -CD, GO,  $\text{Fe}_3\text{O}_4$  and  $\beta$ -CD/MRGO are shown in Fig. 2a. The spectrum of GO shows the existence many oxygen-containing functional groups on the GO surfaces. The peaks at 1034, 1220 and  $1622 \text{ cm}^{-1}$  correspond to C–O stretching vibrations of the epoxy groups, C–OH stretching, and C=C stretching, respectively. The characteristic peak at  $1734 \text{ cm}^{-1}$  corresponds to C=O stretching vibrations of the carboxyl groups, and the peak at  $3440 \text{ cm}^{-1}$  belongs to the O–H stretching vibration. In the IR spectrum of  $\beta$ -CD, the broad band with a maximum at  $3313 \text{ cm}^{-1}$  is ascribed to the stretching vibration of O–H bond in the hydroxy groups. The absorption peak at  $2930 \text{ cm}^{-1}$  belongs to the stretching vibration of C–H bond in the CH and  $\text{CH}_2$  functional groups. The absorption bands in the region  $1204\text{--}1414 \text{ cm}^{-1}$  (1204, 1252, 1296, 1334, 1366 and  $1414 \text{ cm}^{-1}$ ) correspond to the deformation vibration of the O–H bonds in the primary and secondary hydroxy group of  $\beta$ -CD and C–H bending vibrations. The peak at the  $1151 \text{ cm}^{-1}$  is assigned to the coupled C–O–C stretching in the ether and O–H bending vibrations of hydroxy groups. The featured peaks at 1029 and  $1077 \text{ cm}^{-1}$  are attributed to the coupled C–O/C–C stretching and O–H bending vibrations. The absorption peaks at 569, 708, 756

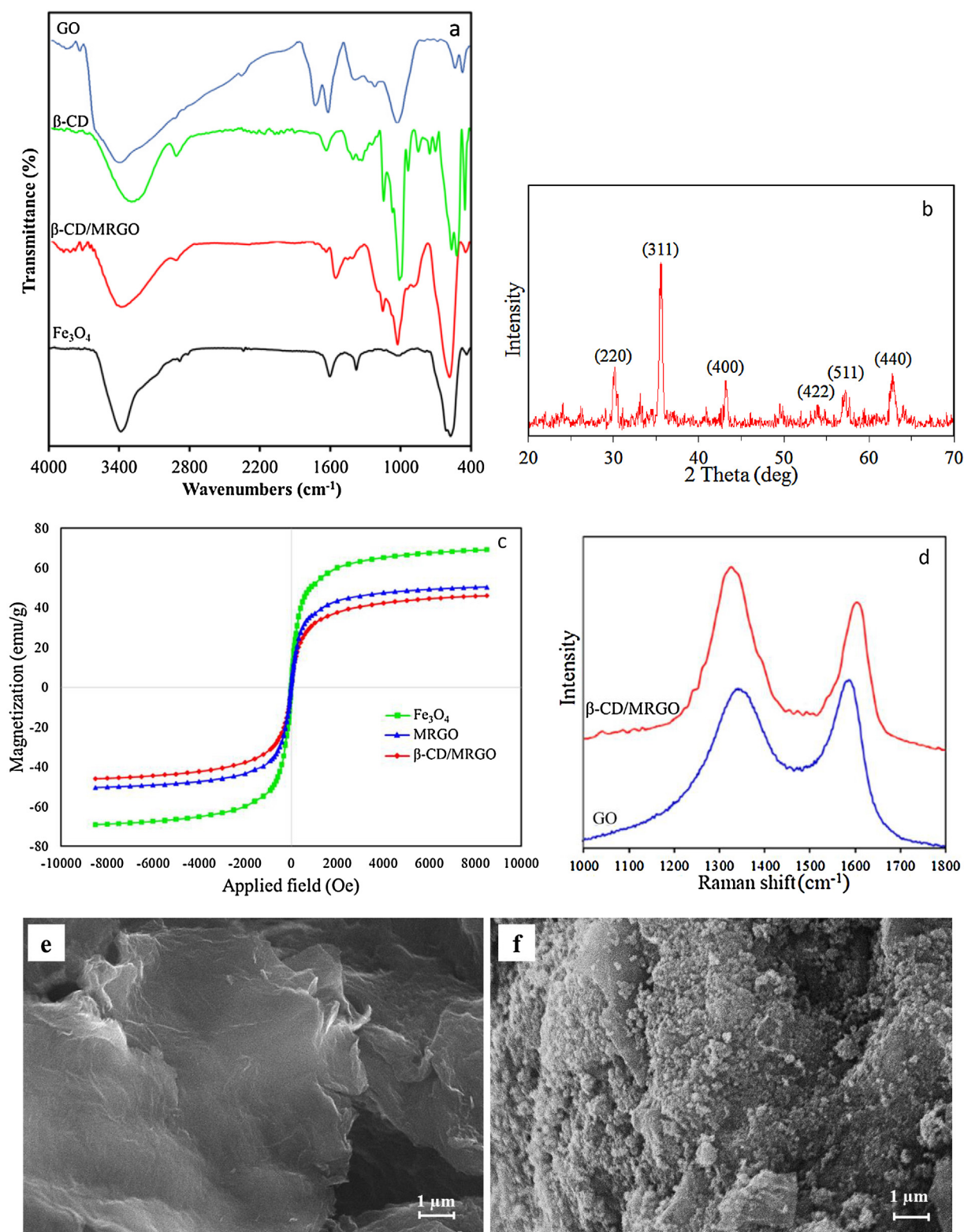


**Fig. 2.** Characterization of materials: (a) FTIR spectra of GO, Fe<sub>3</sub>O<sub>4</sub>, β-CD and β-CD/MRGO; (b) XRD pattern of β-CD/MRGO; (c) room temperature hysteresis loop of Fe<sub>3</sub>O<sub>4</sub>, MRGO and β-CD/MRGO; (d) Raman spectra of GO and β-CD/MRGO; and (e) SEM image of GO and β-CD/MRGO.

and 942 cm<sup>-1</sup> belong to the deformation vibration of the C–H bonds and ring vibration.

The FT-IR spectrum of β-CD/MRGO exhibits typical CD characteristic peaks mentioned above (the absorption peaks at 1029, 1151, 1077, 1414, 2925 and 3429 cm<sup>-1</sup>). This obviously confirms successful attachment of β-CD molecules onto the graphene sur-

faces. The strong peak at 583 cm<sup>-1</sup> in the FT-IR spectrum of β-CD/MRGO, attributed to the Fe–O bond vibration, confirms the existence of Fe<sub>3</sub>O<sub>4</sub> nanoparticles on the structure of nanocomposite. In addition, the C=O vibration band (1740 cm<sup>-1</sup>) disappears due to chemical reduction of GO nanosheets, but the broad O–H and the C–O stretching bands remain.

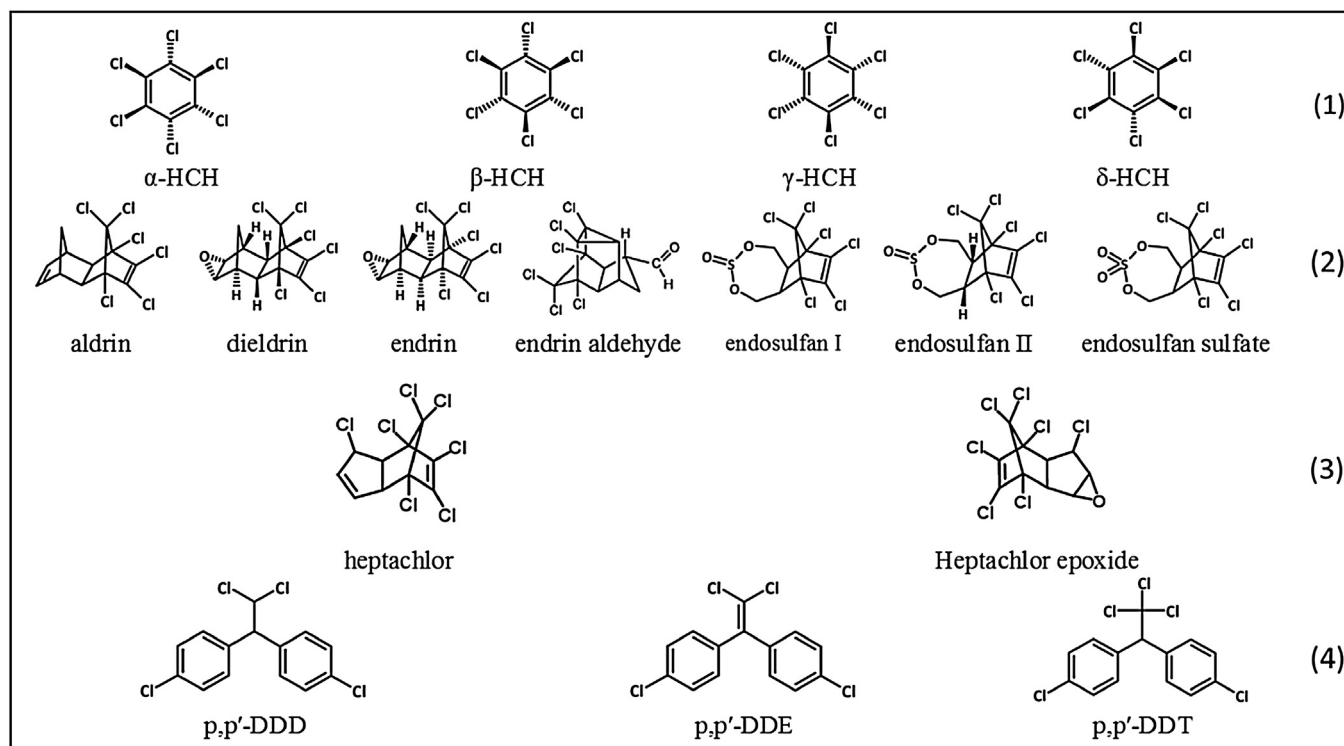


Fig. 3. Structure of investigated OCPs in this study.

The O–H stretching vibration peak at  $3429\text{ cm}^{-1}$  for  $\beta$ -CD/MRGO shows characteristic large red-shift compared with free OH mode (located at about  $3700\text{ cm}^{-1}$ ), indicating the presence of a strong hydrogen bond between  $\beta$ -CD molecules and some oxygen functional groups of GO nanosheets [30]. In fact, only two molecular interactions including hydrophobic interactions and hydrogen-bonding are possible. The hydrophobic cavity of  $\beta$ -CD molecules located inside of the ring. On the other hand, GO nanosheets are in micrometer size. Therefore, the hydrophobic interaction between the cavity of  $\beta$ -CD and GO is not feasible and they can only attach together via strong hydrogen bonding because of multiple oxygen functional groups on the GO surfaces and OH groups of  $\beta$ -CDs. According to the fact described above, the mechanism for fabrication of  $\beta$ -CD/MRGO nanocomposite is considered as follows: the  $\beta$ -CDs would be adsorbed on the surface of GO because of a strong hydrogen bonding between them. At the same time, the ferrous ions ( $\text{Fe}^{2+}$ ) diffuses toward the GO nanosheets through electrostatic interactions, which were then oxidized into ferric ions ( $\text{Fe}^{3+}$ ) effectively by the oxygen-containing functional groups on the GO surfaces. Then, the oxidized  $\text{Fe}^{3+}$  and unoxidized  $\text{Fe}^{2+}$  ions coprecipitated into  $\text{Fe}_3\text{O}_4$  nanoparticles on the GO surfaces under alkaline conditions ( $\text{pH} = 11$ ). The remaining oxygen-containing groups (particularly the OH groups) on the reduced graphene oxide had to continue to form the strong hydrogen bonding with the  $\beta$ -CD molecules.

In order to prove the deposition of  $\text{Fe}_3\text{O}_4$  nanoparticles on the surface of GO, XRD pattern of  $\beta$ -CD/MRGO nanocomposite is shown in Fig. 2b. The diffraction peaks at  $2\theta = 30.2, 35.56, 43.28, 53.24, 57.0$  and  $62.84$  correspond to the (220), (311), (400), (422), (511) and (440) of the cubic spinel crystal planes of  $\text{Fe}_3\text{O}_4$ , respectively. The obtained pattern is consistent with the standard XRD data for bulk  $\text{Fe}_3\text{O}_4$  (Joint Committee on Powder Diffraction Standards, JCPDS, card 19-0629), indicating that  $\text{Fe}_3\text{O}_4$  nanoparticles have been successfully connected with GO nanosheets.

The magnetic properties of  $\text{Fe}_3\text{O}_4$ , MRGO and  $\beta$ -CD/MRGO were investigated by VSM technique at room temperature. As shown in Fig. 2c, the magnetic hysteresis loops of all three samples display S-like curves, which passed through the zero point of magnetization, indicating superparamagnetic properties of these structures. The values of saturation magnetization of  $\text{Fe}_3\text{O}_4$ , MRGO and  $\beta$ -CD/MRGO were  $69.1, 50.4$  and  $46.0\text{ emu g}^{-1}$ , respectively. It is obvious that the saturation magnetizations of MRGO and  $\beta$ -CD/MRGO are lower than bare  $\text{Fe}_3\text{O}_4$ , which can be due to the contribution magnetically inactive GO nanosheets and  $\beta$ -CD molecules to the total magnetization. The saturation magnetization of  $\beta$ -CD/MRGO had a slight decrease compared to MRGO, which clearly confirms the attachment of  $\beta$ -CD on to the reduced graphene nanosheets. However, this amount ( $46.0$ ) is much higher than the enough saturation magnetization value ( $16.3\text{ emu g}^{-1}$ ) reported by Ma et al. [31] for magnetic separation from solution with a magnet. These results indicate that  $\beta$ -CD/MRGO has a good magnetic properties and can be rapidly separated from the sample solution by a magnetic.

Raman spectroscopy was used to characterize the ordered and disordered crystal structures of fabricated  $\beta$ -CD/MRGO. The Raman spectra of GO and  $\beta$ -CD/MRGO are shown in Fig. 2d. The spectrum of GO displays two prominent peaks at about  $1340$  and  $1590\text{ cm}^{-1}$ , which are assigned to the D band (originates from the disorder-induced mode associated with structural defects and imperfections) and G band (corresponds to the first order scattering of the  $\text{E}_{2g}$  phonon of the  $\text{sp}^2$  carbon domains), respectively. The intensity ratio of  $I_D/I_G$  is often applied to measure of disordering. As can be seen, with incorporation  $\beta$ -CD and  $\text{Fe}_3\text{O}_4$  nanoparticles on the RGO surfaces, the  $I_D/I_G$  of  $\beta$ -CD/MRGO shows relative higher intensity than that of GO. These observations suggest a large number of structural defects due to attachment of  $\beta$ -CD and  $\text{Fe}_3\text{O}_4$  to the  $\text{sp}^2$  carbon network.

The SEM micrographs of GO and  $\beta$ -CD/MRGO are shown in Fig. 2e and f, respectively. The differences in the surface morphol-

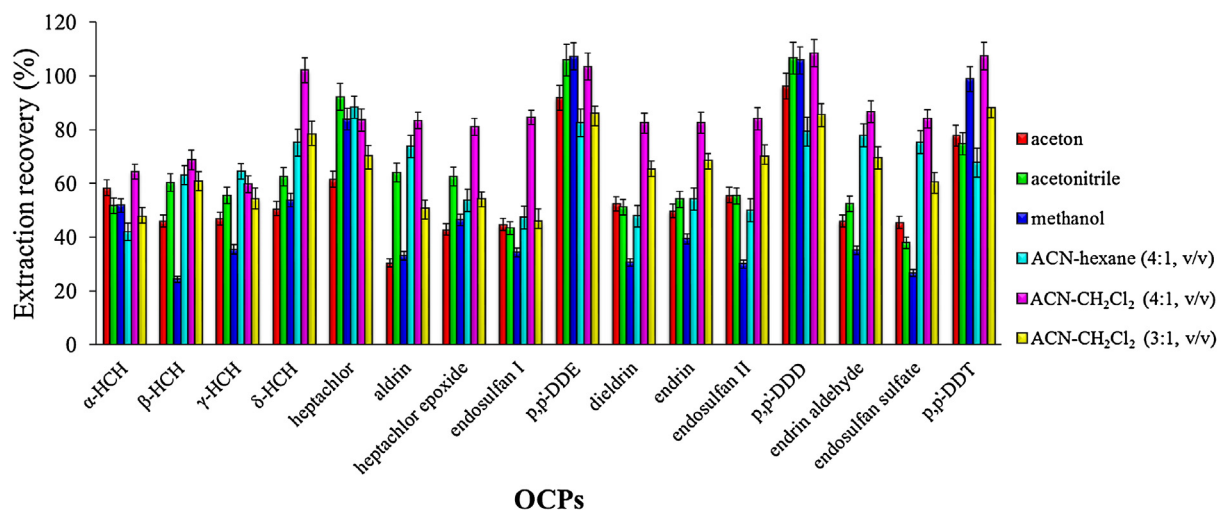


**Fig. 4.** Effect of type of desorption solvent on the OCPs extraction recoveries. Conditions: 500 ng kg<sup>-1</sup> of OCPs, 1 mL of solvent, 2 min of vortex time, 20 mg of adsorbent, pH~6, no salt.

ogy between GO and  $\beta$ -CD/MRGO are clearly observed. As can be seen, the GO has a sheet-like structure with a large thickness, smooth surface, and wrinkled edge while  $\beta$ -CD/MRGO has a much rougher surface, which indicates that many magnetic nanoparticle and  $\beta$ -CD molecules had been assembled on the surface of the GO nanosheets.

The above-mentioned characterization results show the successful synthesis of  $\beta$ -CD/MRGO by a simple one-step hydrothermal reduction strategy which compared to the hydrazine reduction methods and multi-steps procedures, this approach is more simple and non-toxic.

### 3.2. Interaction mechanism between OCPs and $\beta$ -CD/MRGO

The OCPs molecules can interact with the  $\beta$ -CD functionalities on the surfaces of GO nanosheets. The formation of inclusion complex and its binding strength mainly depend on the size/dimension fit and binding forces (such as hydrophobic interactions, van der Waals attractions, hydrogen bonding, electrostatic interactions, etc.) between the host cavity of  $\beta$ -CD and OCPs as guest molecules. The chlorinated pesticides, in this study, had different structure including (1) the hexachlorocyclohexane class ( $\alpha$ -,  $\beta$ -,  $\gamma$ -, and  $\delta$ -HCH), (2) the hexachlorobicycloheptene class (aldrin, dieldrin, endosulfan I, endosulfan II, endosulfan sulfate, endrin, endrin aldehyde), (3) heptachlorobicyclic class (heptachlor, heptachlor epoxide-isomer B), and (4) the p,p' substituted diphenyl class (p,p'-DDE, p,p'-DDD, and p,p'-DDT) as shown in Fig. 3.

As compared to the other classes of pesticides, p,p' substituted diphenyl class can form stronger host-guest complex with  $\beta$ -CD. This may be due to the chemical structure of them, since they have good fit within the cavity of the  $\beta$ -CD functionalities which lead to the formation of stable inclusion complexes. DDT, DDE, and DDD are hydrophobic compounds which contain a symmetrical chlorobenzene ring with the size of 0.2 nm<sup>3</sup>. The  $\beta$ -CD has the same cavity depth and diameter of ~0.78 nm while the volume of its cavity varies between 0.262 and 0.346 nm<sup>3</sup> [32,33]. Therefore, DDT, DDE, and DDD molecules have a characteristic part of chlorobenzene ring that matches into the  $\beta$ -CD cavity. However, highly chlorinated OCPs such as hexachlorocyclohexane and hexachlorobicycloheptene-based class are more difficult to enter into the  $\beta$ -CD cavity owing to their steric hindrance effect.

Since the OCPs are low to moderately polar compounds, the hydrophobic interaction is the main driving force to form the inclu-

sion complex between the OCPs and CD in the aqueous media. Therefore, the pesticides with a higher log P (partition coefficient in *n*-octanol/water) such as DDT, DDE and DDD can be more bound by  $\beta$ -CD cavities. In addition, some of the studied OCPs in this work (such as heptachlor epoxide, endosulfan I and II, endosulfan sulfate, dieldrin, endrin and endrin aldehyde) are H-bond acceptor due to the existence of oxygen atom or carbonyl group on their structures. Therefore, the H-bonding between the oxygen atom/carbonyl group of OCPs and the OH residues at the rime of  $\beta$ -CD may have also contributed to the formation of the  $\beta$ -CD complexes with OCPs.

### 3.3. Optimization of adsorption and desorption conditions

To achieve the best extraction efficiency and obtain optimal MSPE conditions, several parameters including vortex time, amount of adsorbent, pH of sample solution, salt concentration as well as desorption conditions were investigated and optimized. To study the extraction performance, extraction recoveries (R) were used. Recoveries were investigated by analyzing 50 mL of sample solutions spiked with 1000 ng kg<sup>-1</sup> of each OCP. Triplicate measurements were performed at each point and the means of results were used for optimization. Extraction recovery was calculated based on the following equation:

$$\%R = \frac{C_{os} \times V_{os}}{C_{aq} \times V_{aq}} \times 100 \quad (1)$$

where  $C_{os}$  is the analyte concentration in the final organic solvent,  $C_{aq}$  is the initial concentration of the analyte in the aqueous phase and  $V_{os}$  and  $V_{aq}$  are the volumes of final organic solvent and the aqueous phase, respectively.

#### 3.3.1. Effect of desorption conditions

Effective desorption of extracted analytes from the surface of adsorbent by a suitable solvent is an important step. Sufficient elution and good extraction efficiency can be achieved by both the proper dispersion of the magnetic adsorbent in the solvent and capability of solvent to extract target analytes. Owing to hydrophilic nature of  $\beta$ -CD/MRGO and existence polar groups on the structure of adsorbent, it can be dispersed well in a polar solvent. On the other hand, a nonpolar solvent may be more suited to desorb OCPs from the adsorbent surface due to the low or moderate polarity of them, but the aggregation of  $\beta$ -CD/MRGO nanoparticles will occur, discouraging the extraction procedure.

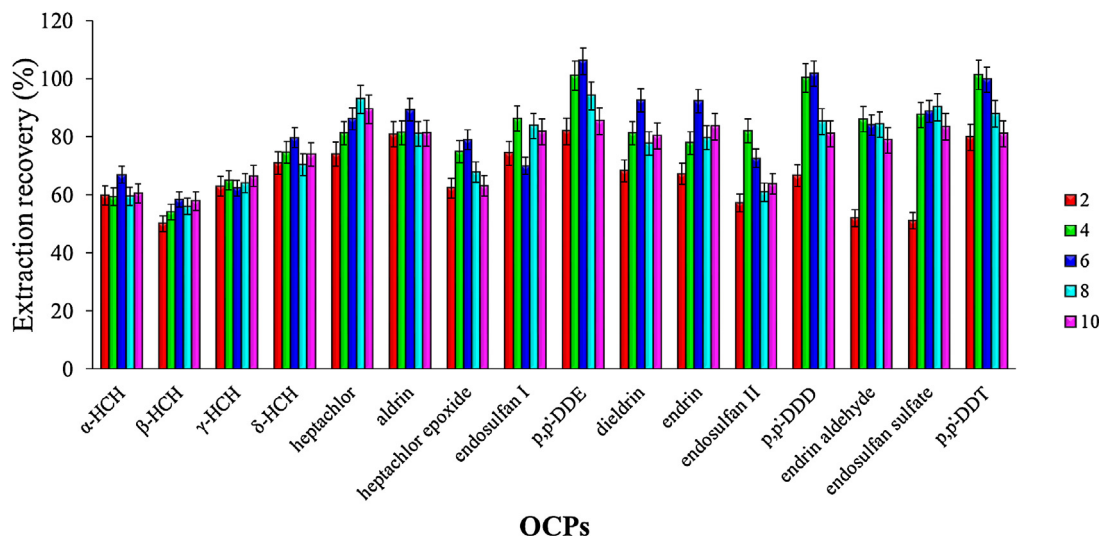


**Fig. 5.** Effect of sample solution pH on the OCPs extraction recoveries. Conditions: 500 ng kg<sup>-1</sup> of OCPs, 1 mL of acetonitrile-dichloromethane (4:1, v/v), 3 min of vortex time, 20 mg of adsorbent, no salt.

The other important factor that should be considered when selecting a suitable solvent for desorption of analytes is the insolubility of impurities in the solvent. Co-eluting compounds from the sample matrix can affect the signal of analytes by a signal enhancement or suppression. These unfavorable effects may lead to a decrease in accuracy, precision, and sensitivity of the method.

In the current work, different organic solvents containing methanol, acetone, acetonitrile, acetonitrile-hexane (4:1, v/v), acetonitrile-dichloromethane (4:1, v/v) and acetonitrile-dichloromethane (3:1, v/v) were selected as desorption solvent, and their extraction efficiencies were compared.

According to the results shown in Fig. 4 methanol had poor eluting capability compared with the other elution solvents. Acetone and acetonitrile showed better extraction recoveries for p,p'-DDE, p,p'-DDD, and p,p'-DDT than methanol, but they had poor desorption ability for other compounds. The mixture of acetonitrile-hexane showed a better extraction recoveries for some OCPs, but it exhibited a low extraction efficiency for some compounds, such as heptachlor epoxide, dieldrin, endrin, p,p'-DDT, p,p'-DDD and p,p'-DDE. Using acetonitrile-dichloromethane (4:1, v/v) as the desorption solvent, the highest extraction recoveries were obtained. The lower extraction recoveries obtained for acetonitrile-dichloromethane (3:1, v/v) could be attributed to the weaker dispersability of the adsorbent in the solvent by decreasing the mixture polarity. This may be lead to poor penetration of the solvent to the surfaces of adsorbent and agglomeration of the adsorbent nanosheets that can decrease the specific surface area and hinder the effective desorption of analytes. According to the above discussion, acetonitrile-dichloromethane (4:1, v/v) was chosen as the best desorption solvent.

The volume of desorption solvent is also a key factor to obtain reliable and reproducible analytical results. Therefore, the influence of desorption solvent volume on the OCPs extraction recoveries was studied with different volume of acetonitrile-dichloromethane (4:1, v/v). It was found that the greatest extraction recoveries can be achieved with elution the adsorbent by 0.5 mL acetonitrile-dichloromethane (4:1, v/v) for two times. Hence, the total amount of 1 mL (2 × 0.5 mL) of acetonitrile-dichloromethane (4:1, v/v) was selected for desorption of OCPs from the β-CD/MRGO.

The effect of desorption time was also investigated by increasing the vortex duration from 0.5 to 3 min the results (not shown) showed that no significant changes were observed for the extrac-

tion recoveries of OCPs after 0.5 min of vortex time. Thus, the vortex time of 1 min was selected to insure complete desorption of analytes from the adsorbent.

### 3.3.2. Effect of dilution factor

Since honey has a complex matrix and the pesticides distribute in the sample between a “free” and a “bound” form with matrix components, a sample dilution can increase the extraction efficiencies due to matrix effect reduction. But, excess dilution of samples is unfavorable for a trace analysis. Therefore, it is necessary to choose a proper dilution factor. In this study, the effect of dilution factor was investigated by analyzing 50 mL water sample containing different weights of OCP free honey (10, 5, 3, 2, 1 and 0.5 g) spiked at 1000 ng kg<sup>-1</sup> of OCPs. The results (not shown) indicated that the highest extraction recoveries for all OCPs were achieved for 50 mL water containing 2 g of honey (a 25-fold dilution) and further dilution had not significant effect on the enhancement of extraction recoveries. Hence, 2 g of honey dissolved in 50 mL water was adopted for further experiments.

### 3.3.3. Effect of vortex time

In MSPE procedures, extraction time is an important factor which can affect the extraction efficiency. To obtain the satisfactory adsorption equilibrium, sufficient contact time between the adsorbent and analytes is required. Mass transfer of analytes to adsorbent can be increased with the agitation of sample solution due to a decrease in the thickness of diffusion film with agitation. In this study, different vortex times (1, 2, 3, 4, and 5 min) were studied after dispersing the adsorbent into the sample solution by means of vortex agitator at 3000 rpm. On the basis of obtained results, all extraction recoveries were increased by extending the vortex time from 1 to 3 min while longer times slightly reduced the extraction recoveries. The same experiments were also performed by shaking the sample solution with a platform shaker as well as ultrasonication for comparison with the use of vortex mixing. The results (data not shown) demonstrated that the use of vortex provided shorter equilibrium time compared to shaker (15 min) and ultrasonication (8 min). The obtained rapid equilibrium can be explained by the fact that the adsorbent can be uniformly dispersed into the sample solution by the aid of vortex agitator, making the contact area between the adsorbent and the OCPs molecules large enough for a fast mass transfer. Based on the results of above, the vortex time

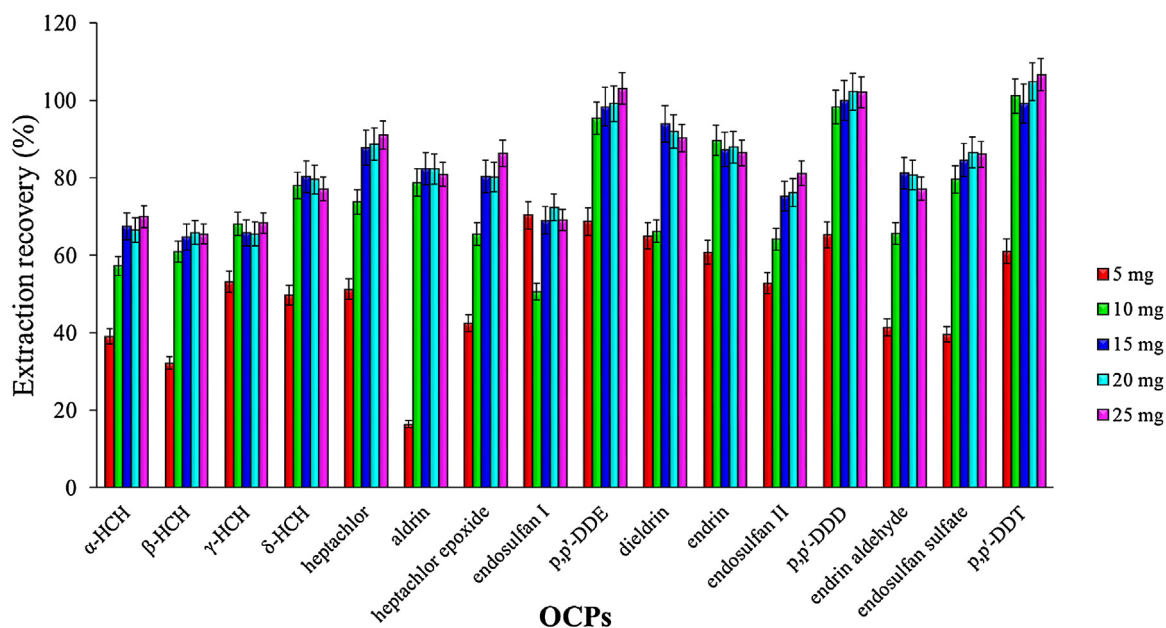


**Fig. 6.** Effect of adsorbent amount on the OCPs extraction recoveries. Conditions: 500 ng kg<sup>-1</sup> of OCPs, 1 mL of acetonitrile-dichloromethane (4:1, v/v), 3 min of vortex time, pH=6, no salt.

of 3 min was selected for the optimum extraction time in the next steps.

### 3.3.4. Effect of pH of the sample

The sample solution pH can affect the extraction efficiency in a MSPE procedure by altering the chemical forms of analytes and/or surface charge of the adsorbent. Thus, the effect of solution pH on the OCPs extraction recoveries was investigated by adjusting pH from 2 to 10 with HCl or NaOH while other experimental conditions were kept constant. Fig. 5 shows that the extraction recoveries of the analytes remained almost constant at pH values between 4.0 and 8.0; when the pH was lower than 4.0 or higher than 8.0, the extraction recoveries of some compound were decreased. This was probably due to the fact that some of the OCPs are degraded during the acid or base hydrolysis step [34]. Under very acidic medium, some compound such as dieldrin, endrin and heptachlor epoxide can be degraded into its dechlorinated products and diol derivative. On the other hand, some OCPs, including DDT, DDD and DDE may slowly hydrolyzed under basic conditions. In addition, the oxygen groups on the adsorbent are ionized (carrying negative charge) at alkaline conditions and thus adsorb more water molecules which blocks the access of OCPs molecules to the adsorption sites of CD/MRGO and results in the reduction of extraction recoveries. Therefore, extremely acidic or basic conditions should be avoided in the sample preparation steps. Since the pH of the investigated honey samples after dilution were in the range of 5–7, there was no need to adjust the pH of the sample solution.

### 3.3.5. Effect of adsorbent amount

The adsorbent amount had a significant effect on extraction efficiency. Low amount of adsorbent is not sufficient to the effective extraction of analytes from the sample solution. On the other hand, high amount of adsorbent cannot improve the extraction efficiency and may require a higher amount of eluent solvent to desorb the analytes. In this work, the effect of the adsorbent amount was studied by varying the amount of β-CD/MRGO from 5 to 25 mg. As shown in Fig. 6, the extraction recoveries for all OCPs increased as the amount of adsorbent increased. In the amounts of adsorbent more than 15 mg, the extraction recoveries remained almost

constant, indicating that 15 mg of adsorbent was sufficient to the effective extraction of OCPs from the sample solution. According to the result, 15 mg of β-CD/MRGO was used in the following studies.

### 3.3.6. Effect of salinity

In general, a suitable ionic strength can decrease the solubility of the analytes in an aqueous media and therefore enhancing their partitioning into the organic phase. The effect of salt on the extraction recoveries of OCPs using β-CD/MRGO was investigated by adding different amounts of NaCl ranging from 0 to 7% (w/v). As illustrated in Fig. 7, the extraction recoveries for all OCPs were increased with addition of salt up to 3% w/v. When the salt content was further increased to 5%, the extraction recoveries were decreased for some OCPs, and with more amount of salt (7%) all extraction recoveries were decreased. It can be explained by the fact that the sodium ions can form inclusion complex with β-CD cavity, and thus at high salt content, the bonded sodium ions reduce interaction sites on the surface of β-CD/MRGO with OCPs which result in the lower extraction recoveries. In addition, high ionic strength can limit the molecular transfer rate to the surfaces of the adsorbent due to increase the viscosity of bulk solution. Based on the above results, 3% (w/v) of NaCl was used as optimum salt concentration for other experiments.

## 3.4. Reusability and reproducibility of adsorbent

Regeneration and reuse of adsorbent are very important aspect of the SPE-base procedure from economy and environmental point of view. The ability to reuse of adsorbent can reduce the need for new adsorbent and the problem of waste of used adsorbent which make the treatment method more economical and environmental friendly. In order to investigate the reusability of the prepared adsorbent, after desorption of the analytes from the surfaces of β-CD/MRGO completed, it was washed with acetone and water, and then reused for the next MSPE procedure according to section 2.5. The results showed that the adsorbent can be reused at least 15 times without significant loss of the extraction recoveries (<10%) of OCPs. This fact indicates that β-CD/MRGO has a great potential for repeated use in sample preparation.



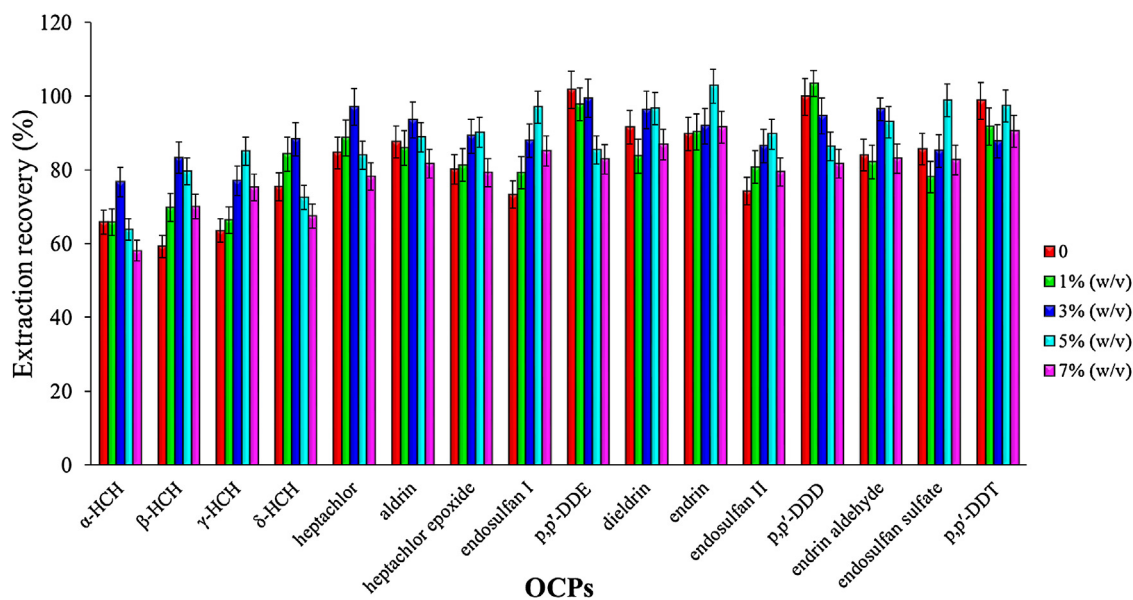


**Fig. 7.** Effect of salt concentration on the OCPs extraction recoveries. Conditions: 500 ng kg<sup>-1</sup> of OCPs, 1 mL of acetonitrile-dichloromethane (4:1, v/v), 3 min of vortex time, 15 mg of adsorbent, pH~6.

The reproducibility of the material is considered as a key factor in the evaluation of the proposed vortex-assisted-MSPE performance. To evaluate the reproducibility of the synthesized  $\beta$ -CD/MRGO nanocomposite for MSPE, a 50 mL of sample solution containing OCPs spiked at 50 ng kg<sup>-1</sup> was extracted with  $\beta$ -CD/MRGO nanocomposite using the described MSPE in section 2.5. Five portions (15 mg) of  $\beta$ -CD/MRGO that had been prepared in one batch was selected to give the intra-batch relative standard deviations (RSDs), and the inter-batch RSDs were obtained by means of the adsorbents that had been independently prepared over three batches (five replicates analysis for each adsorbent). The mean recoveries were also compared with Tukey test at  $p < 0.05$ . The intra- and inter-batch RSDs were obtained in the ranges of 4.1% and 6.6% respectively and no significant difference in the mean recoveries was observed. The results indicated that the adsorbent had satisfactory reproducibility for OCPs extraction.

### 3.5. Validation of the method and real sample analysis

To evaluate the performance of the developed vortex-assisted-MSPE/GC-ECD method for the analysis of the OCPs, analytical parameters including linear dynamic ranges (LDRs), determination coefficients ( $R^2$ ), limits of detection (LODs), limits of quantification (LOQs), preconcentration factors (PFs) and precisions were determined under the optimized experimental conditions.

A series of blank water samples spiked with OCPs standards at different concentration levels and honey sample solutions spiked at the same levels were prepared to establish the standard and matrix-matched calibration curves, respectively. For each level, three replicate extractions and determinations were performed and the calibration curve of each OCP was constructed by plotting the peak areas versus the corresponding concentration of the analytes. To evaluate the effect of matrix, the difference in slopes and determination coefficients of both calibration curves (matrix matched calibration and standard calibration) was investigated using one-way ANOVA at significant level of 5% for each analyte. The results showed that there was no significant difference between the two curves indicating no observable matrix effect (Table S1, supplementary information). However, for an accurate quantification, a matrix-matched calibration was used and the results were summarized in Table 1. The limits of detection (LODs) and quantification

(LOQs) of the method were calculated at the signal to noise ratio of 3 ( $S/N=3$ ) and 10 ( $S/N=3$ ), respectively. Preconcentration factor (PF) was defined as the ratio of the analyte concentration in the organic phase to its initial concentration in the source phase.

Repeatability and reproducibility of the method were evaluated in terms of intra-day and inter-day precisions, respectively. The intra-day and inter-day precisions were investigated by the extraction and determination of the analytes from the spiked honey samples at 50 ng kg<sup>-1</sup> of each OCP (five times) in the same day and the same process (five replicate) on three consecutive days. The results expressed as the relative standard deviation (RSD), are shown in Table 1. As can be seen, the acceptable precisions were obtained indicated that the proposed method is sensitive and repeatable.

In order to evaluate the applicability of the proposed method, it was used for determination of the OCPs in honey samples. For this purpose, three labels of honey (one natural honey labeled as honey 1 and two commercial honey labeled as honey 2 and honey 3), with different origins were prepared from local supermarkets (Tehran, Iran). Each honey sample (2 g) was mixed with 50 mL deionized water and stirred with a vortex mixer for few minutes to form a homogeneous solution. As no reference materials was available for honey, the accuracy of the method was verified with recovery tests by analyzing the honey samples spiked at 50 and 500 ng kg<sup>-1</sup> of OCPs standards. The results are shown in Table 2. The acceptable obtained recoveries from 78.8% to 116.2%, with low RSDs (below 8.1%) demonstrated the applicability of the developed MSPE method based on  $\beta$ -CD/MRGO for the determination of OCPs in honey samples. The representative chromatograms of honey samples analysis are shown in supplementary information, Fig. s1.

### 3.6. Comparison with other extraction methods

The performance of the proposed method was compared with other previously reported SPE based methods for analysis OCPs in honey [12,35–41]. The results in Table 3 showed that the MSPE method based on  $\beta$ -CD/MRGO as adsorbent, provided good analytical features in term of LOD, accuracy (as%recovery) and precision (as%RSD). The results were better or comparable to the other reported methods. Very low LODs in the sub-part per trillion (sub-

**Table 1**  
Analytical performance data for the OCPs analysis in honey by the proposed MSPE method.

No.	OCPs	LDR (ng kg <sup>-1</sup> )	R <sup>2</sup>	LOD (ng kg <sup>-1</sup> )	LOQ (ng kg <sup>-1</sup> )	RSDs (%)		PF
						Intraday (n = 5)	Inter-day (n = 15)	
1	α-HCH	2–5000	0.9981	0.61	2.03	3.3	5.7	373
2	β-HCH	2–5000	0.9992	0.68	2.27	2.9	6.2	386
3	γ-HCH	2–5000	0.9997	0.74	2.46	3.2	4.6	390
4	δ-HCH	2–5000	0.9985	0.75	2.50	3.8	6.6	431
5	heptachlor	2–5000	0.9996	0.75	2.50	4.2	7.8	485
6	aldrin	2–5000	0.9970	0.67	2.23	6.6	7.0	467
7	heptachlor epoxide	2–5000	0.9992	0.69	2.30	4.0	5.6	445
8	endosulfan I	2–5000	0.9988	0.65	2.17	3.7	4.5	439
9	p,p'-DDE	2–5000	0.9995	0.52	1.73	5.1	4.4	506
10	dieldrin	2–5000	0.9994	0.65	2.17	4.6	7.2	481
11	endrin	3–5000	0.9966	0.85	2.83	4.5	6.9	459
12	endosulfan II	3–5000	0.9978	0.87	2.90	3.7	6.4	432
13	p,p'-DDD	3–5000	0.9979	0.73	2.43	5.8	7.1	493
14	endrin aldehyde	5–5000	0.9972	1.45	4.83	4.2	5.2	482
15	endosulfan sulfate	10–10000	0.9969	3.21	10.72	4.3	6.3	425
16	p,p'-DDT	10–10000	0.9991	3.12	10.42	4.9	6.5	488

**Table 2**  
Results for the analysis of OCPs in honey.

OCPs	Honey 1			Honey 2			Honey 3		
	Found (ng kg <sup>-1</sup> )	R <sup>a</sup> (RSD) (%)	R <sup>b</sup> (RSD) (%)	Found (ng kg <sup>-1</sup> )	R <sup>a</sup> (RSD) (%)	R <sup>b</sup> (RSD) (%)	Found (ng kg <sup>-1</sup> )	R <sup>a</sup> (RSD) (%)	R <sup>b</sup> (RSD) (%)
α-HCH	10.1	80.4 (3.2)	78.8 (4.2)	–	88.9 (5.7)	91.3 (5.2)	–	85.4 (4.6)	92.9 (5.4)
β-HCH	–	88.5 (4.6)	85.9 (5.3)	–	91.5 (4.4)	89.0 (7.2)	–	93.7 (7.2)	82.1 (4.7)
γ-HCH	19.4	79.7 (3.8)	91.4 (4.8)	–	86.7 (4.5)	88.6 (3.9)	–	94.2 (5.3)	84.6 (5.1)
δ-HCH	–	87.0 (3.9)	93.2 (6.0)	–	97.2 (3.8)	92.5 (5.4)	–	84.5 (4.1)	87.0 (7.5)
heptachlor	–	92.7 (4.4)	89.5 (4.7)	–	88.9 (5.1)	93.7 (4.5)	–	91.6 (5.8)	95.3 (3.2)
aldrin	–	98.6 (5.6)	88.8 (3.8)	–	92.1 (4.0)	82.7 (6.8)	–	87.3 (5.5)	91.7 (5.3)
heptachlor epoxide	–	101.0 (3.9)	80.0 (4.2)	–	94.6 (7.6)	92.4 (4.8)	–	89.1 (4.7)	93.4 (4.6)
endosulfan I	13.3	85.6 (4.7)	101.1 (6.8)	–	90.3 (4.9)	86.9 (5.0)	–	93.5 (4.4)	88.2 (5.0)
p,p'-DDE	–	104.1 (5.3)	94.2 (5.1)	–	97.4 (4.6)	92.1 (4.7)	–	95.9 (5.8)	103.6 (4.3)
dieldrin	–	93.2 (2.9)	92.2 (4.8)	–	84.7 (6.5)	87.2 (5.1)	–	92.8 (6.0)	89.7 (5.3)
endrin	–	95.6 (6.1)	82.6 (3.5)	–	91.8 (5.2)	93.8 (3.7)	–	88.0 (4.3)	92.5 (4.9)
endosulfan II isomer B	–	89.7 (4.8)	84.9 (5.4)	–	93.0 (6.2)	83.5 (4.3)	–	94.2 (4.9)	90.1 (4.9)
p,p'-DDD	–	106.0 (6.4)	94.1 (4.8)	–	111.1 (3.7)	96.9 (6.1)	–	102.3 (5.6)	95.7 (3.8)
endrin aldehyde	–	94.3 (5.5)	88.7 (4.9)	–	89.2 (4.3)	95.6 (7.3)	–	85.1 (5.7)	87.8 (5.6)
endosulfan sulfate	–	88.8 (4.9)	96.9 (8.1)	–	85.6 (5.1)	102.0 (5.6)	–	93.4 (4.2)	94.3 (6.0)
p,p'-DDT	–	98.5 (5.2)	99.7 (3.7)	–	103.4 (5.4)	92.3 (4.4)	–	97.6 (3.8)	116.2 (4.1)

<sup>a</sup>Recovery, spike at 50 ng kg<sup>-1</sup><sup>b</sup>Recovery, spike at 500 ng kg<sup>-1</sup>**Table 3**  
Comparison of the proposed MSPE method with other SPE-based techniques for determination of OCPs in honey.

Method	Adsorbent type	LOD (μg kg <sup>-1</sup> )	Extraction time (min)	Recovery (%)	RSD (%)	Adsorbent Amount (mg)	Ref.
SPE-GC/ECD	Florisil	0.4–2	–	77.31–105.22	–	2000	[35]
SPE-GC/ECD	C <sub>18</sub> octadecyl	0.05–0.2	–	48–125	2–13	360	[36]
SPE-GC/MS	C <sub>18</sub> octadecyl	3–20	–	79–98	3–18	500	[37]
SPE-GC/FPD	EXTrelut NT 20	0.2–8.0	–	66–93	2–19	–	[38]
DSPE <sup>a</sup> -GC/ECD	PSA <sup>b</sup>	20–50	–	80.7–114.5	2.5–21.9	400	[39]
SPE-GC/ECD	SPE-Visiprep DL	0.1–0.6	–	63.4–94	5–15	–	[40]
SPME-GC/AED <sup>c</sup>	PDMS/PA <sup>d</sup>	0.02–0.08	20	Average 91.4	7.5–11.3	–	[12]
MSPE-GC/ECD	CoFe <sub>2</sub> O <sub>4</sub> -MWCNTs	1.3–3.6 (ng L <sup>-1</sup> )	40	83.2–128.7	2.1–6.4	10	[41]
MSPE-GC/ECD	β-CD/MRGO	0.0005–0.0032	3	78.8–116.2	3.3–7.8	15	This work

<sup>a</sup>Dispersive solid phase extraction.<sup>b</sup>Primary secondary amine bulk sorbent.<sup>c</sup>Atomic emission detection.<sup>d</sup>PDMS: Polydimethylsiloxane, PA: Polyacrylate.

ppt) to ppt range for the proposed method were obviously considerable in comparison with other methods. The rapidity was the other significant benefit of the presented method that was the result of combining direct addition of adsorbent to the sample solution and vortex agitator, leading to increase the contact between the adsorbent and analytes. This also makes the SPE procedure easier to treatment of large sample volumes and avoiding channeling or blocking of cartridges. In addition, the amount of adsorbent was considerably low in compared with SPE techniques which is an

important benefit as it greatly reduced the analysis cost. These results confirmed that this method is a very fast, sensitive, reliable and efficient sample preparation technique for OCPs analysis.

#### 4. Conclusion

In this research, a novel and simple approach was successfully developed to synthesis of β-CD/magnetic reduced graphene oxide hybrid composite in one step using nontoxic reagents. The analysis

results of XRD, SEM, FT-IR, Raman and VSM indicated the successful synthesis of  $\beta$ -CD/MRGO nanocomposite. The prepared nanocomposite was then employed as adsorbent for analysis of the OCPs residues in honey using a vortex-assisted MSPE method. Large surface-to-volume ratio of GO, magnetic convenience separation of adsorbent and strong supramolecular recognition and enrichment capability of  $\beta$ -CD molecules resulted in developing a simple and fast sample preparation method for OCPs extraction with good analytical features (acceptable extraction recovery, very low detection limits and satisfactory repeatability and reproducibility). The rapidity of the method was due to the combination of direct addition of the adsorbent to the solution and using vortex agitator that extremely increases the contact area between the adsorbent and analytes. Moreover, the nanomaterial could be easily regenerated and reused several times without loss of extraction recoveries that is an important issue in SPE-based techniques in term of economy and environment friendly. Owing to the non-polar characteristic of OCPs, the main driving force for the molecular binding on  $\beta$ -CD/MRGO was a hydrophobic interaction for the formation of the OCPs inclusion complexes with  $\beta$ -CDs. The shape/size selectivity of DDT and its metabolites (DDD and DDE) was also responsible for the molecular recognition by the  $\beta$ -CD/MRGO. The results demonstrated that the vortex-assisted MSPE based on  $\beta$ -CD/MRGO hybrid composite can be used as a valuable tool for extraction and pre-concentration of the ultra-trace levels (sub- ppt to ppt) of OCPs residues in honey samples. The  $\beta$ -CD/MRGO hybrid nanomaterial can also offer promising application potential as a biocompatible and nontoxic green sorbent for separation/enantioseparation of other organic contaminants during environmental pollution pre-treatments.

## Appendix A. Supplementary data

Supplementary data associated with this article can be found, in the online version, at <http://dx.doi.org/10.1016/j.chroma.2017.01.035>.

## References

- [1] R. Zhao, X. Wang, J. Yuan, T. Jiang, S. Fu, X. Xu, A novel headspace solid-phase microextraction method for the exact determination of organochlorine pesticides in environmental soil samples, *Anal. Bioanal. Chem.* 384 (2006) 1584–1589.
- [2] D.V. Moreno, Z.S. Ferrera, J.J.S. Rodríguez, Microwave assisted micellar extraction coupled with solid phase microextraction for the determination of organochlorine pesticides in soil samples, *Anal. Chim. Acta* 571 (2006) 51–57.
- [3] M.C. Vagi, A.S. Petsas, M.N. Kostopoulou, M.K. Karamanoli, T.D. Lekkas, Determination of organochlorine pesticides in marine sediments samples using ultrasonic solvent extraction followed by GC/ECD, *Desalination* 210 (2007) 146–156.
- [4] C. Cortada, L. Vidal, R. Pastor, N. Santiago, A. Canals, Determination of organochlorine pesticides in water samples by dispersive liquid–liquid microextraction coupled to gas chromatography–mass spectrometry, *Anal. Chim. Acta* 649 (2009) 218–221.
- [5] A.G. Frenich, J.L.M. Vidal, M.M. Frías, F. Olea-Serrano, N. Olea, L.C. Rodriguez, Determination of organochlorine pesticides by GC-ECD and GC-MS-MS techniques including an evaluation of the uncertainty associated with the results, *Chromatographia* 57 (2003) 213–220.
- [6] R. Rial-Otero, E.M. Gaspar, I. Moura, J.L. Capelo, Chromatographic-based methods for pesticide determination in honey: an overview, *Talanta* 71 (2007) 503–514.
- [7] S.R. Rissato, M.S. Galhiane, F.R.N. Knoll, B.M. Apon, Supercritical fluid extraction for pesticide multiresidue analysis in honey: determination by gas chromatography with electron-capture and mass spectrometry detection, *J. Chromatogr. A* 1048 (2004) 153–159.
- [8] T. Elements, C. Sanchez-Brunete, B. Albero, E. Miguel, J.L. Tadeo, Determination of insecticides in honey by matrix solid-phase dispersion and gas chromatography with nitrogen-phosphorus detection and mass spectrometric confirmation, *J. AOAC Int.* 85 (2002) 128–133.
- [9] C. Blasco, C.M. Lino, Y. Picó, A. Pena, G. Font, M.I.N. Silveira, Determination of organochlorine pesticide residues in honey from the central zone of Portugal and the Valencian community of Spain, *J. Chromatogr. A* 1049 (2004) 155–160.
- [10] M. Volante, R. Galarini, V. Miano, M. Cattaneo, I. Pecorelli, M. Bianchi, et al., A SPME-GC-MS approach for antivarroa and pesticide residues analysis in honey, *Chromatographia* 54 (2001) 241–246.
- [11] M.W. Kujawski, E. Pinteaux, J. Namieśnik, Application of dispersive liquid–liquid microextraction for the determination of selected organochlorine pesticides in honey by gas chromatography–mass spectrometry, *Eur. Food Res. Technol.* 234 (2011) 223–230.
- [12] N. Campillo, R. Peñalver, N. Aguinaga, M. Hernández-Córdoba, Solid-phase microextraction and gas chromatography with atomic emission detection for multiresidue determination of pesticides in honey, *Anal. Chim. Acta* 562 (2006) 9–15.
- [13] L.T. Adeo, Analysis of pesticides in honey by solid-phase extraction and gas chromatography–mass spectrometry, *J. Agric. Food Chem.* (2004) 5828–5835.
- [14] Y. Liu, H. Li, J.-M. Lin, Magnetic solid-phase extraction based on octadecyl functionalization of monodisperse magnetic ferrite microspheres for the determination of polycyclic aromatic hydrocarbons in aqueous samples coupled with gas chromatography–mass spectrometry, *Talanta* 77 (2009) 1037–1042.
- [15] B.T. Zhang, X. Zheng, H.-F. Li, J.-M. Lin, Application of carbon-based nanomaterials in sample preparation: a review, *Anal. Chim. Acta* 784 (2013) 1–17.
- [16] D.A. Dikin, S. Stankovich, E.J. Zimney, R.D. Piner, G.H.B. Dommett, G. Evmenenko, et al., Preparation and characterization of graphene oxide paper, *Nature* 448 (2007) 457–460.
- [17] G. Petrovic, G. Stojanovic, O. Jovanovic, A. Djordjevic, I. Palic, S. Sovilj, Inclusion complexes of pesticides in aqueous solutions of methylated- $\beta$ -cyclodextrin, *Hem. Ind.* 67 (2013) 231–237.
- [18] T. Tian, F. Qiu, K. Dong, D. Yang, Application of an inclusion complex for determination of dithianon residues in water and fruits, *Toxicol. Environ. Chem.* 94 (2012) 1034–1042.
- [19] J. Wu, P. Su, D. Guo, J. Huang, Y. Yang, Cationic  $\beta$ -cyclodextrin-modified hybrid magnetic microspheres as chiral selectors for selective chiral absorption of dansyl amino acids, *New J. Chem.* 38 (2014) 3630–3636.
- [20] D. Wang, L. Liu, X. Jiang, J. Yu, X. Chen, Adsorption and removal of malachite green from aqueous solution using magnetic  $\beta$ -cyclodextrin–graphene oxide nanocomposites as adsorbents, *Colloids Surf. A: Physicochem. Eng. Asp.* 466 (2015) 166–173.
- [21] L. Li, L. Fan, M. Sun, H. Qiu, X. Li, H. Duan, et al., Adsorbent for chromium removal based on graphene oxide functionalized with magnetic cyclodextrin–chitosan, *Colloids Surf. B: Biointerfaces* 107 (2013) 76–83.
- [22] W. Song, D. Shao, S. Lu, X. Wang, Simultaneous removal of uranium and humic acid by cyclodextrin modified graphene oxide nanosheets, *Sci. China Chem.* 57 (2014) 1291–1299.
- [23] S. Wang, Y. Li, X. Fan, F. Zhang, G. Zhang,  $\beta$ -Cyclodextrin functionalized graphene oxide: an efficient and recyclable adsorbent for the removal of dye pollutants, *Front. Chem. Sci. Eng.* 9 (2016) 77–83.
- [24] W. Song, J. Hu, Y. Zhao, D. Shao, J. Li, Efficient removal of cobalt from aqueous solution using  $\beta$ -cyclodextrin modified graphene oxide, *RSC Adv.* 3 (2013) 9514–9521.
- [25] Y. Guo, S. Guo, J. Li, E. Wang, S. Dong, Cyclodextrin–graphene hybrid nanosheets as enhanced sensing platform for ultrasensitive determination of carbendazim, *Talanta* 84 (2011) 60–64.
- [26] C. Wang, B. Li, W. Niu, S. Hong, B. Saif, S. Wang, et al.,  $\beta$ -Cyclodextrin modified graphene oxide–magnetic nanocomposite for targeted delivery and pH-sensitive release of stereoisomeric anti-cancer drugs, *RSC Adv.* 5 (2015) 89299–89308.
- [27] L. Fan, C. Luo, M. Sun, H. Qiu, Synthesis of graphene oxide decorated with magnetic cyclodextrin for fast chromium removal, *J. Mater. Chem.* 22 (2012) 24577–24583.
- [28] R. Liang, C. Liu, X. Meng, J. Wang, J. Qiu, A novel open-tubular capillary electrochromatography using  $\beta$ -cyclodextrin functionalized graphene oxide–magnetic nanocomposites as tunable stationary phase, *J. Chromatogr. A* 1266 (2012) 95–102.
- [29] S. Mahpishanian, H. Sereshti, Graphene oxide-based dispersive micro-solid phase extraction for separation and pre-concentration of nicotine from biological and environmental water samples followed by gas chromatography–flame ionization detection, *Talanta* 130 (2014) 71–77.
- [30] Y. Guo, S. Guo, J. Ren, Y. Zhai, S. Dong, E. Wang, Cyclodextrin functionalized graphene nanosheets with high supramolecular recognition capability: synthesis and host–guest inclusion for enhanced electrochemical performance, *ACS Nano* 4 (2010) 4001–4010.
- [31] Z. Ma, Y. Guan, H. Liu, Synthesis and characterization of micron-sized monodisperse superparamagnetic polymer particles with amino groups, *J. Polym. Sci. Part A: Polym. Chem.* 43 (2005) 3433–3439.
- [32] T. Uyar, R. Havelund, J. Hacıoğlu, F. Besenbacher, P. Kingshott, Cyclodextrins: comparison of molecular filter performance, *ACS Nano* 4 (2010) 5121–5130.
- [33] J. Zhang, M. Pan, N. Gan, Y. Cao, D. Wu, Employment of a novel magnetically multifunctional purifying material for determination of toxic highly chlorinated polychlorinated biphenyls at trace levels in soil samples, *J. Chromatogr. A* 1364 (2014) 36–44.
- [34] M.S. Kim, T.W. Kang, H. Pyo, J. Yoon, K. Choi, J. Hong, Determination of organochlorine pesticides in sediment using graphitized carbon black solid-phase extraction and gas chromatography/mass spectrometry, *J. Chromatogr. A* 1208 (2008) 25–33.

- [35] H. Yavuz, G.O. Guler, A. Aktumsek, Y.S. Cakmak, H. Ozparlak, Determination of some organochlorine pesticide residues in honeys from Konya Turkey, *Environ. Monit. Assess.* 168 (2010) 277–283.
- [36] D. Tsipi, M. Triantafyllou, A. Hiskia, Determination of organochlorine pesticide residues in honey, applying solid phase extraction with RP-C18 material, *Analyst* 124 (1999) 473–475.
- [37] C. Blasco, M. Fernández, A. Pena, C. Lino, M.I. Silveira, G. Font, et al., Assessment of pesticide residues in honey samples from Portugal and Spain, *J. Agric. Food Chem.* 51 (2003) 8132–8138.
- [38] G. Amendola, P. Pelosi, R. Dommarco, Solid-phase extraction for multi-residue analysis of pesticides in honey, *J. Environ. Sci. Health. B* 46 (2011) 24–34.
- [39] A.A. Barakat, H.M.A. Badawy, E. Salama, E. Attallah, G. Maatook, Simple and rapid method of analysis for determination of pesticide residues in honey using dispersive solid phase extraction and GC determination, *J. Food. Agric. Env.* 5 (2007) 97–100.
- [40] A. Herrera, C. Pérez-Arquillué, P. Conchello, S. Bayarri, R. Lázaro, C. Yagüe, et al., Determination of pesticides and PCBs in honey by solid-phase extraction cleanup followed by gas chromatography with electron-capture and nitrogen-phosphorus detection, *Anal. Bioanal. Chem.* 381 (2005) 695–701.
- [41] Z. Du, M. Liu, G. Li, Novel magnetic SPE method based on carbon nanotubes filled with cobalt ferrite for the analysis of organochlorine pesticides in honey and tea, *J. Sep. Sci.* 36 (2013) 3387–3394.